IEEE Access
Multidisciplinary | Rapid Review | Open Access Journal

Received October 22, 2021, accepted November 1, 2021, date of publication November 9, 2021,
date of current version November 18, 2021.

*Digital Object Identifier 10.1109/ACCESS.2021.3126872*

# An Evaluation Framework for Second-Life EV/PHEV Battery Application in Power Systems

**SONGJIAN CHAI[1,2], (Member, IEEE), NING ZHOU XU[3], (Member, IEEE), MING NIU[4], KA WING CHAN[5], (Member, IEEE), CHI YUNG CHUNG[6], (Fellow, IEEE), HUI JIANG[2], AND YUXIN SUN[7]**

[1]College of Physics and Optoelectronic Engineering, Shenzhen University, Shenzhen 518060, China
[2]College of Mechatronics and Control Engineering, Shenzhen University, Shenzhen 518060, China
[3]Experimental Power Grid Centre, Energy Research Institute @ NTU, Nanyang Technological University, Singapore 627590
[4]Electric Power Research Institute, State Grid Liaoning Electric Power Company Ltd., Shenyang, Liaoning 110006, China
[5]Department of Electrical Engineering, The Hong Kong Polytechnic University, Hong Kong
[6]Department of Electrical and Computer Engineering, University of Saskatchewan, Saskatoon, SK S7N 5A9, Canada
[7]Department of Electrical Engineering and Electronics, University of Liverpool, Liverpool L69 7ZX, U.K.

Corresponding authors: Hui Jiang (huijiang@szu.edu.cn) and Ning Zhou Xu (11901711r@connect.polyu.hk)

This work was supported in part by the Energy Market Authority and the National Research Foundation Singapore under Grant NRF2017EWT-EP003-038, in part by the National Key Research and Development Program of China under Grant 2019YFB1505400, and in part by the Foundation of Shenzhen Science and Technology Committee under Grant GJHZ20180928160212241 and Grant JCYJ20190808165201648.

**ABSTRACT** Energy storage is essential for balancing the generation and load in power systems. Building a battery energy storage system (BESS) with retired battery packs from electric vehicles (EVs) or plug-in hybrid electric vehicles (PHEVs) is one possible way to subsidize the price of EV/PHEV batteries, and at the same time mitigating forecast error introduced by load and renewable energy sources in power systems. This paper proposes a detailed framework to evaluate end-of-life (EOL) EV/PHEV batteries in BESS application. The framework consists of three parts. A generalized model for battery degradation is first introduced. It is followed by modeling the battery retirement process in its first life. Two vehicle types—EV and PHEV—as well as two retirement modes—nominal and realistic modes—are considered. Finally, the application of the second-life BESS in power systems is modeled in a detailed economic dispatch (ED) problem. This is how second-life BESS's performance translates into cost savings on power generation. An optimization problem is formulated to maximize total cost savings in power generation over the battery's second life. This is done by striking a balance between short-term benefit (daily cost savings) and long-term benefit (cost savings through service years). Numerical results validate the effectiveness of the proposed framework/models. They show that battery usage and retirement criterion in its first life directly affect the performance in its second life application. In our case study, EV battery packs possess larger EOL energy capacities and consequently generate more cost savings in the second life. However, the BESS built from retired PHEV batteries has higher cost savings per MWh. It is because, with the proposed degradation model, battery health is better preserved in PHEV applications. Compared to nominal retirement mode, realistic retirement mode results in extra cost savings due to the reduced first-life service years.

**INDEX TERMS** Battery degradation, battery energy storage system (BESS), battery repurposing, economic dispatch (ED), electric vehicle (EV), end-of-life (EOL), forecast error, plug-in electric vehicle (PHEV), second-life application, used-battery.

## NOMENCLATURE

### A. VARIABLES

| | |
|---|---|
| $C^0_{2\text{nd},i}$ | Relative capacity of battery pack $i$ at the beginning of its second life. |
| $D$ | Depth of discharge. |
| $d$ | Day counter. |
| $E_{\text{R},i}$ | Rated energy capacity of battery pack $i$. |
| $L_{1\text{st},i}$ | Life expectancy of battery pack $i$ in EV/PHEV. |
| $L_{\text{A},i}$ | Actual life span of battery pack $i$ in EV/PHEV. |
| $N_d$ | Number of cycles within day $d$. |
| $n$ | Cycle number. |

The associate editor coordinating the review of this manuscript and approving it for publication was Hao Wang.

| | |
|---|---|
| $P_j^t$ and $P_j^{t'}$ | Power output of generator $j$ at hour $t$ without and with BESS. |
| $P_{\mathrm{FE}}^t$ | Total forecast error at hour $t$. |
| $P_{\mathrm{FL}}^t$ | Forecast load at hour $t$. |
| $P_{\mathrm{WTG,R}}$ | Rated capacity of WTGs. |
| $P_{\mathrm{WTG}}^t$ | Power output of WTGs at hour $t$. |
| $v_{\mathrm{W}}^t$ | Wind speed at hour $t$. |
| $\Delta E_{\mathrm{2nd},i}^t$ | Energy contributed from battery pack $i$ in BESS at hour $t$. |
| $\Delta E_{\mathrm{BESS}}$ | Daily operating energy capacity for the BESS. |
| $\Delta E_{\mathrm{2nd},i}^d$ | Average energy contribution of battery pack $i$ in BESS during day $t_{\mathrm{d}}$. |
| $\eta_{\mathrm{2nd},i}^0$ | Efficiency of battery pack $i$ at the beginning of its second life. |

### B. FUNCTIONS

| | |
|---|---|
| $C(.)$ | Relative capacity. |
| $C_{\mathrm{1st},i}^n(.)$ | Relative capacity at cycle $n$ of battery pack $i$ in EV/PHEV. |
| $C_{\mathrm{2nd},i}^d(.)$ | Relative capacity of battery pack $i$ in BESS at the end of day $d$. |
| $c_{\mathrm{saving}}(.)$ | Function of total cost savings. |
| $c_{\mathrm{total},j}(.)$ | Cost function of generator $j$. |
| $R(.)$ | Changes of relative internal resistance. |
| $\eta(.)$ | Efficiency. |
| $\eta^0(.)$ | Initial efficiency of a battery pack. |
| $\eta_{\mathrm{1st},i}^n$ | Efficiency at cycle $n$ of battery pack $i$ in EV/PHEV. |
| $\eta_{\mathrm{2nd},i}^d(.)$ | Efficiency of battery pack $i$ in BESS at the end of day $d$. |

### C. PARAMETERS

| | |
|---|---|
| $F_{\mathrm{E}}$ | Emission factor. |
| $k_{0,j}$, $k_{1,j}$ and $k_{2,j}$ | Constants of the quadratic heat rate function for generator $j$. |
| $M_i$ | Average daily mileage of EV $i$. |
| $M_{\mathrm{T}}$ | Total mileage for EV. |
| $N_{\mathrm{CD}}$ | Minimum number of cycles for CD mode. |
| $N_{\mathrm{CS}}$ | Minimum number of cycles for CS mode. |
| $N_{\mathrm{G}}$ | Number of generators. |
| $N_{\mathrm{V}}$ | Number of battery packs in BESS. |
| $p_{\mathrm{coal}}$ | Coal price. |
| $p_{\mathrm{CO_2}}$ | $CO_2$ price. |
| $T_d$ | The period of day $d$. |
| $v_{\mathrm{CO}}$, $v_{\mathrm{CI}}$ and $v_{\mathrm{R}}$ | Cut-in, cut-out and rated speed of WTGs. |
| $\sigma_{\mathrm{FE}}$ | Standard deviation of total forecast error. |
| $\sigma_{\mathrm{LE}}$ | Standard deviation of load forecast error. |
| $\sigma_{\mathrm{WE}}$ | Standard deviation of wind power forecast error. |
| $\eta_{\mathrm{PCS}}$ | Efficiency of the power conversion system (PCS) of BESS. |

### D. SETS

| | |
|---|---|
| $\mathbf{S_{Batt}}$ | Set of operating conditions for battery packs in the BESS. |
| $\mathbf{S_{BESS}}$ | Set of operating conditions for the BESS. |

## I. INTRODUCTION

Energy storage is essential for balancing the generation and load. With the proliferation of renewable energy sources (RES) worldwide, the need for storage increases remarkedly in recent years. Despite the increasing market foothold of electric vehicles (EVs) and plug-in hybrid electric vehicles (PHEVs) in recent years, the price remains the most significant hurdle against EVs' popularization. Bringing down the costs is essential to have long-term commercial viability [1]. On the other hand, end-of-life (EOL) battery disposal becomes an emerging issue. Repurposing retired EV/PHEV battery provides a potential way to reduce the cost hurdle while alleviating environmental concerns over EOL battery disposal [2]. In power systems, battery energy storage systems (BESS) can be built from EOL batteries and provide services. It is due to the fact that EOL batteries can still meet the requirement for the less-demanding grid services [3]. Building a BESS with second-life EV/PHEV batteries is especially appealing as the increasing RES capacity in power systems calls for more spinning reserves [4].

### A. LITERATURE REVIEW

Economic and technical aspects of EOL EV/PHEV battery and its second-life applications have been studied over the last two decades [1]–[3], [5]–[16]. Among the existing literature, potential economic benefits and business models for post-vehicle battery applications are discussed extensively. Comprehensive studies on the feasibility of applying used EV batteries in stationary applications are given by Sandia National Laboratories [10] and National Renewable Energy Laboratory [11], [13]. Application considered spans from transmission support, area regulation, and spinning reserve to renewable firming load leveling. Williams and Lipman [12], [17] explore repurposing battery packs for stationary use as a way to reduce battery-lease payment. Potential business models of second-life EV batteries are reported in [2] and [7]. In [15], the economic viability is assessed based on electricity tariffs across three countries. In [11], the initial purchase price of second-life EV/PHEV batteries is calculated based on net present value. Simplified economic analysis for frequency regulation service is carried out in [1], where various scenarios are studied regarding the state of health (SOH) and rates for regulation service. Recently, thorough reviews are given by Martinez-Laserna *et al.* on second-life applications of lithium-ion batteries [3], [9].

For specific applications, modeling both battery and second-life applications are required. Several works of literature provide insights in this regard. Li *et al.* [6] design a real-life test framework for second-life EV batteries

in a residential application. For the same application, a MATLAB-Simulink model is proposed in [5]. Alimisis and Hatziargyriou [14] study the case in the island of Crete (non-interconnected), where used EV batteries are deployed to complement wind power. In [18], various ways for modeling Li-ion batteries considering battery SOH in grid-scale applications are reviewed. Experimental tests on used EV batteries are reported in [8], [19]. Economic analyses on second-life EV batteries in applications such as renewable smoothing are presented in [20], [21], and [22].

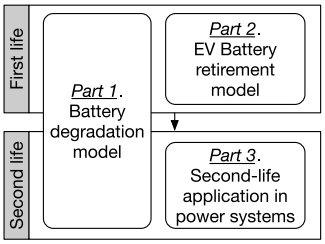


**FIGURE 1.** Framework for study on second-life battery applications.

A general framework for second-life battery application is given in Figure 1. The modeling work involved is threefold: 1. Battery degradation model, 2. Battery retirement model and 3. Modeling of the second-life application. As outlined in the figure, Part 1 decides how battery performance degrades over time. Part 2 determines at what stage the battery is retired and repurposed. Finally, a technical/economic assessment for the second-life application is carried out in Part 3. Depending on the specific scope of work, the complexity of the model in each part can vary.

In prevailing studies, the focus is business models and economic viability across different second-life applications (i.e., Part 3 in Figure 1). For those studies, the battery degradation process (i.e., Part 1) is often not elaborated. Instead, fixed life expectancy is assumed. In modelling battery retirement process (i.e., Part 2), simple criterion for first-life retirement are applied, such as fixed energy capacity [7], [12], [14], [17], [23]. For second-life application (i.e., Part 3), economic feasibility is assessed with given tariff structures. This is suitable for scenarios in which the stakeholder of repurposed batteries is the price taker. However, storage systems' operation has a direct impact on power generation's planning and operation. It is especially true in systems where intermittent generation sources' share is higher, and storage is required to lower the level of risk resulting from the intermittency [24], [25]. Consequently, the cost of power generation is heavily affected by both generators and storage systems in such systems and needs to be considered. To summarize, the existing literature focuses only on one or two parts of the three-part framework, leaving the remaining as simple assumptions.

### B. CONTRIBUTION OF THIS WORK

In this paper, a comprehensive evaluation framework is proposed for EV/PHEV batteries' second-life application in power systems. In this framework, all three parts (in Figure 1) are taken into considered and modeled. It answers the question of how battery degradation and retirement in the vehicle can affect its second-life BESS application and subsequently translate into cost savings on the power generation side.

With the rising share of intermittent RES and increasing load in power systems, it gets challenging to get accurate predictions for their power output and demand [26]–[28]. This paper is the first to envision BESS made from EOL batteries to be used to absorb forecast error of wind power and load (i.e., Part 3 in Figure 1). The operation of the second-life battery is integrated into a detailed generation scheduling (economic dispatch) problem. Maximum cost savings throughout the second life is achieved by balancing charging/discharging depth and service years in the second life. The battery degradation process is modeled (i.e., Part 1), accounting for performance deterioration. In modeling battery retirement (i.e., Part 2), first-life usage patterns as well as retirement criteria are considered for both PHEV and EV types. Two battery retirement modes are considered: nominal and realistic modes. Normally, battery packs are retired upon they fail to meet certain technical criteria [29]. However, it is usual that in practicing vehicle retirement or change of ownership can take place earlier [30]. If collected at this stage, the repurposed battery will exhibit different EOL performances.

The organization of this paper is as follows. A simplified model for measuring battery performance degradation is introduced in Section II (corresponding to Part 1 in Figure 1), followed by retirement models for EV and PHEV battery packs in Section III (i.e., Part 2 in Figure 1). Based on these models, the status of battery packs at the commencement of their second-life application can be determined. The operating strategy of the BESS is proposed in Section IV (i.e., Part 3 in Figure 3). An economic dispatch (ED) problem is then formulated. In Section V, numerical testing is studied. Section VI concludes the paper.

## II. MODELING BATTERY PERFORMANCE DEGRADATION

Given the myriad types of cathodes and electrolytes and requirements for model complexities, currently, there is no single presiding degradation model for lithium batteries [11], [31]–[35]. However, general degradation patterns can be extracted with simplification assumptions. In this paper, a simplified model for battery performance degradation are generalized from [32]–[34], [36].

### A. CAPACITY FADE

Field tests and research works have revealed that the energy capacity fade of modern batteries strongly depends on the number of cycles, depth of discharge (DoD), C-rate, and ambient temperature [32]–[34], [37]. Among these variables, the temperature is often regarded as a given condition under which the cycle life tests are carried out [34], [33], [32]. For EV/PHEV batteries, typical C-rate profiles reflecting driving

patterns are also provided [32]–[34], [38]. Consequently, the remaining energy capacity of the batteries in per-unit value, i.e., relative capacity, can be simplified as a function of cycle number and DoD:

$$C(n, D) \tag{1}$$

As the number of cycles accumulates monotonously and serves as a type of "timestamp" in batteries' life, in the remainder of this paper "$n$" is represented by superscript instead. i.e.

$$C^n(D) = C(n, D)$$

Without loss of generality, superscripts in this paper are reserved for chronological variables such as cycle number $n$, hour $t$, and day count $n$.

General degradation trend and boundary conditions are given by (2)–(6), when the ambient temperature is around 35°C [32]–[34], [37]:

$$C^n(0\%) = 1.0 \tag{2}$$

$$C^0(D) = 1.0 \tag{3}$$

$$\frac{\partial}{\partial n} C^n(D) \leq 0 \tag{4}$$

$$\frac{\partial}{\partial D} C^n(D) \leq 0 \tag{5}$$

$$\frac{\partial}{\partial n'} C^{n'}(D) \geq \frac{\partial}{\partial n''} C^{n''}(D) \quad \forall n' < n'' \tag{6}$$

0% DoD results in zero degradation, (2), either does 0 cycle number, (3). Monotonicity in performance degradation is depicted by (4) and (5) with regard to the number of cycles and DoD, respectively. Battery capacity either reduces or stays at the same level with any given $n$, i.e. (4), and $D$, i.e. (5). The other general observation is that capacity fade normally speeds up over time, as provided in (4). As the number of cycles accumulates, capacity loss between cycles also increases.

A linear relationship can be found between DoD ($D$) and the logarithm of cycle number ($\log(n)$), [34]. Using the techniques of curve and surface fitting [39], [40], relative capacity can be represented by a function of cycle number and DoD as:

$$C^n(D) = 1 - \left(a \cdot n \cdot 10^{b \cdot (D-1)}\right)^{-\frac{1}{c}} \tag{7}$$

where $a$, $b$ and $c$ are designated constants. (7) is consistent with condition (2)–(6). Its proof is presented in Appendix-A.

### B. EFFICIENCY DECAY

Approximate linear relationships can be observed between internal loss and cycle number and between internal loss and DoD [32]–[34]. Also, the slope of the linear relationship between internal loss and cycle number increases with DoD. As external circuits have much greater resistance than the internal, the percent increase in internal loss is assumed to equate to percent efficiency decay.

The efficiency function is given by:

$$\eta^n(D) = \eta(n, D) = 1 - \left(1 + R^n(D)\right)\left(1 - \eta^0(D)\right) \tag{8}$$

where

$$R^n(D) = \frac{(\alpha_1 \cdot D + \beta_1) \cdot n}{\alpha_2 \cdot D + \beta_2} \tag{9}$$

$$\eta^0(D) = \alpha_3 \cdot D + \beta_3 \tag{10}$$

and $\alpha_1$–$\alpha_3$ and $\beta_1$–$\beta_3$ are designated constants; $\alpha_1 / \alpha_3$ should be equal to $(\beta_3 - 100\%) / \beta_2$. With (8)—(10), the above efficiency decay trend can be met. Its proof is detailed in Appendix-B.

It should be noted that although a generalized degradation model for lithium-ion batteries is used in this paper, our proposed framework can adopt any degradation model by replacing the above (1)—(10) if battery type or requirements for model complexity change. The whole evaluation process for second-life battery in this paper holds as long as battery capacity fade and efficiency decay can be estimated.

## III. BATTERY RETIREMENT MODES IN EV/PHEV

EOL battery status is heavily dependent upon the usage pattern and the service duration in its vehicle application. However, currently, it is not certain at what stage EV/PHEV batteries are retired and repurposed. In this paper, two vehicle retirement modes—nominal and realistic modes—are considered alongside the vehicle types. Nominal retirement mode describes the situation where batteries are recycled when they reach their technical EOL conditions. Realistic retirement mode considers the fact that vehicles are often retired before they are technically retired.

### A. NOMINAL RETIREMENT MODE–EOL FOR PHEV BATTERY PACK

Technical EOL are defined by consortiums such as USABC [29]. For example, it is compulsory for a PHEV battery pack to last for 5,000 cycles in charge depleting (CD) mode and 300,000 cycles in charging sustaining (CS) mode [29]. The initial battery status for its second-life application is then the EOL condition in PHEV. EOL capacity and efficiency are given in (11) and (12), respectively. In this paper, subscripts "1st" and "2nd" are used to indicate first and second-life applications of battery, respectively.

$$C^0_{2\text{nd},i} = \min\left\{C^{N_{\text{CD}}}_{1\text{st},i}(\Delta E_{\text{CD}}), C^{N_{\text{CS}}}_{1\text{st},i}(\Delta E_{\text{CS}})\right\} \tag{11}$$

$$\eta^0_{2\text{nd},i} = \min\left\{\eta^{N_{\text{CD}}}_{1\text{st},i}(\Delta E_{\text{CD}}), \eta^{N_{\text{CS}}}_{1\text{st},i}(\Delta E_{\text{CS}})\right\} \tag{12}$$

where $\Delta E_{\text{CD}}$ and $\Delta E_{\text{CS}}$ are required energy for CD and CS modes, respectively. For example, $\Delta E_{\text{CD}}$ is 11.6 kWh for a 20.7 kWh PHEV battery pack and $\Delta E_{\text{CS}}$ is 0.5 kWh [29]. Total cycle numbers and DoD that are nominally required for CD and CS modes are first applied to degradation model (1)—(10). The EOL status is then determined by either CD or CS mode, whichever results in lower values, thus min in (11) and (12).

When calculating the EOL, one thing worth noticing is the DoD definition. DoD is usually given in percentage value. In some test results, the denominator of DoD is the rated energy capacity of the battery, which is a constant. In some other test results, the DoD value is based on actual energy capacity, which is a variable that decreases along with the cycle test. If the latter DoD definition is used when modeling battery degradation, cycle-to-cycle iterations should be carried out to calculate relative capacity and efficiency. In each cycle, the DoD base needs to be updated.

### B. NOMINAL RETIREMENT MODE–EOL FOR EV BATTERY PACK

EOL relative capacity and efficiency for EV battery pack are given by (13) and (14), respectively.

$$C^0_{2\text{nd},i} = C^{n_{\max}}_{1\text{st},i}(\Delta E_i) \tag{13}$$

$$\eta^0_{2\text{nd},i} = \eta^{n_{\max}}_{1\text{st},i}(\Delta E_i) \tag{14}$$

where $\Delta E_i$ is energy requirement incurred by daily travel mileage $M_i$ and is given by (18), assuming daily mileage for each EV $i$ are constant.

Different from PHEV, battery is the only energy source for EV propulsion. As a result, the battery $i$ would be retired when its energy capacity is no longer able to deliver the daily travel mileage requirement, i.e., violation of (15), assuming the consumption rate of EV is 0.20 kWh/mile,

$$M_i \geq \frac{E_{\text{R},i} \cdot C^n_{1\text{st},i}(\Delta E_i) \cdot \eta^n_{1\text{st},i}(\Delta E_i)}{0.20\text{kWh/mile}} \tag{15}$$

Besides, it could also be retired once EV's nominal EOL mileage $M_{\text{T}}$ is reached, i.e., violation of (16):

$$M_i \cdot n \leq M_{\text{T}} \tag{16}$$

Substituting (13) and (14) into (15), the maximum cycle number $n_{\max}$ is determined by the comparison between the above two conditions (15) and (16):

$$n_{\max} = \min\left\{ \frac{M_{\text{T}}}{M_i}, n \,\middle|\, M_i = \frac{E_{\text{R},i} \cdot C^n_{1\text{st},i}(\Delta E_i) \cdot \eta^n_{1\text{st},i}(\Delta E_i)}{0.20} \right\} \tag{17}$$

where $\Delta E_i$ can be calculated with given $M_i$, assuming each EV completes 1 cycle every day:

$$\Delta E_i = M_i \cdot 0.20 \tag{18}$$

### C. REALISTIC RETIREMENT MODE

In the real world, it is usual that vehicle retirement or change of ownership takes place before it is technically retired. The length of vehicle ownership in the United States averages 11.6 years while 6.6 years for new vehicle ownership [30]. After the first ownership ends, EV/PHEV can be repurposed at a low cost.

For PHEV application, it can be regarded charge depleting and charge sustaining cycles are deployed with a same frequency over its life span. The number of cycles used in CD or CD mode is thus proportional to the actual life in the vehicle application.

$$C^0_{2\text{nd},i} = \min\left\{ C^{\left(\frac{L_{\text{A},i}}{L_{1\text{st},i}} \cdot N_{\text{CD}}\right)}_{1\text{st},i}(11.6)\,, C^{\left(\frac{L_{\text{A},i}}{L_{1\text{st},i}} \cdot N_{\text{CS}}\right)}_{1\text{st},i}(0.5) \right\} \tag{19}$$

$$\eta^0_{2\text{nd},i} = \min\left\{ \eta^{\left(\frac{L_{\text{A},i}}{L_{1\text{st},i}} \cdot N_{\text{CD}}\right)}_{1\text{st},i}(11.6)\,, \eta^{\left(\frac{L_{\text{A},i}}{L_{1\text{st},i}} \cdot N_{\text{CD}}\right)}_{1\text{st},i}(0.5) \right\} \tag{20}$$

Similarly, (17) can be replaced by (21) for EV application.

$$n_{\max} = \frac{L_{\text{A},i}}{L_{1\text{st},i}} \cdot \min\left\{ \frac{M_{\text{T}}}{M_i}, n \,\middle|\, M_i = \frac{E_{\text{R},i} \cdot C^{n_{\max}}_{1\text{st},i}(\Delta E_i) \cdot \eta^{n_{\max}}_{1\text{st},i}(\Delta E_i)}{0.20} \right\} \tag{21}$$

## IV. COST-SAVING EVALUATION FOR BESS MITIGATING FORECAST ERROR

Battery can be used for many applications in power systems [25], [41]–[44], from regulation service [45]–[47] to load balancing [48]. Among them, applications requiring frequent charging and discharging such as regulation service can wear second-life BESS down quickly as recycled battery packs may already be in unhealthy conditions. Applications with long duration and large energy discharge such as peak shaving are not acceptable as well since deep DoDs can also make the battery deteriorate seriously.

For second-life battery, two main applications are residential demand response and power smoothing renewable integration [9], [21], [22]. In this paper, the latter is considered. With wind power penetration escalating nowadays, the unavoidable errors caused by wind power forecasts and load forecast can significantly affect the system operation. The second-life BESS can mitigate the effects of such errors while maintaining its battery performance by properly choosing the time window and energy capacity for operation.

### A. OPERATING STRATEGY OF THE BESS

In this paper, BESS operation is integrated into daily EDs with an hourly time window. With BESS absorbing forecast error of wind power and load, the total cost for power generation is reduced. The more energy is used for each charge/discharge cycle, the more cost savings will incur. However, deeper DoD might also accelerate the degradation, hence reduce the total savings over its service life.

Here, a decision variable called daily operating energy capacity for BESS ($\Delta E_{\text{BESS}}$) is introduced. $\Delta E_{\text{BESS}}$ specifies the total daily amount of energy charged into or discharged from the second-life BESS for the purpose of forecast error mitigation. For illustration, Figure. 2(a) shows a typical distribution of forecast error. As the distribution has the mean of zero [28], the chances of battery charging and discharging are even in the long run. An error-duration curve can be collected for either positive or negative error, as exemplified

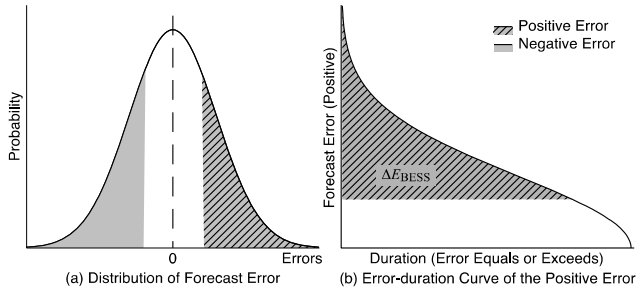


**FIGURE 2.** Illustration for the error-duration curve.

in Figure. 2(b). $\Delta E_{\text{BESS}}$ thus designates a fixed area in the power-time plane. Since it directly links to the forecast errors to be mitigated during the day as well as the DoD, $\Delta E_{\text{BESS}}$ represents the trade-off between daily cost savings and service life of the BESS. The generation scheduling problem is formulated to determine the optimal $\Delta E_{\text{BESS}}$, with which maximum cost savings can be achieved.

### B. PROBLEM FORMULATION

The total cost savings made by second-life BESS lies in the balance between daily cost savings and service life. The total cost savings is the sum of the daily cost savings throughout the service life of the BESS. It is a function of $\Delta E_{\text{BESS}}$, as charging/discharging affects ED scheduling. Determining $\Delta E_{\text{BESS}}$ poses a decision problem. For instance, higher $\Delta E_{\text{BESS}}$ could mean higher daily cost savings, but BESS's service life may shorten; lower $\Delta E_{\text{BESS}}$, on the other hand, does not necessarily interpret into lower total cost savings since service life can be extended.

BESS operation is to maximize the total cost savings. Relative capacities and efficiencies of battery packs can be regarded as constant during the day and degradation takes place between days. So, battery status is updated on a daily basis, same as ED. The optimization problem is formulated as follows:

$$\begin{aligned} &\textit{Maximize}: c_{\text{saving}}\left(\Delta E_{\text{BESS}}\right) \\ &\quad = \sum\nolimits_{t=1}^{\mathbf{S_{BESS}}} \sum\nolimits_{j=1}^{N_{\text{G}}} \left(c_{\text{total},j}\left(P_j^t\right) - c_{\text{total},j}\left(P_j^{t'}\right)\right) \end{aligned} \tag{22}$$

$$\begin{aligned} &\textit{subject to}: c_{\text{total},j}\left(P_j^t\right) \\ &\quad = \left(p_{\text{coal}} + p_{\text{CO}_2}\right) \\ &\quad \cdot \left(k_{0,j} + k_{1,j} \cdot P_j^t + k_{2,j} \cdot \left(P_j^t\right)^2\right) \end{aligned} \tag{23}$$

$$\sum_{j=1}^{N_{\text{G}}} P_j^t = P_{\text{FL}}^t - P_{\text{WTG}}^t + P_{\text{FE}}^t \tag{24}$$

$$0 \le \Delta E_{\text{BESS}} \le \sum_{i=1}^{N_{\text{V}}} C_{2\text{nd},i}^0 \tag{25}$$

$$\Delta E_{\text{BESS}} = \sum_{t_{\text{d}}^{\Delta t}} \sum_{i=1}^{N_{\text{V}}} \left|\Delta E_{2\text{nd},i}^t\right|, \forall E_{2\text{nd},i}^t < 0 \tag{26}$$

$$\Delta E_{\text{BESS}} = \sum_{t}^{\Delta t_{\text{d}}} \sum_{i=1}^{N_{\text{V}}} \Delta E_{2\text{nd},i}^t, \forall E_{2\text{nd},i}^t > 0 \tag{27}$$

$$\begin{aligned} &1\text{h} \cdot \sum_{t}^{T_{\text{d}}} \sum_{j=1}^{N_{\text{G}}} \frac{\left(P_j^t - P_j^{t'}\right)}{\eta_{\text{PCS}} \cdot \eta_{2\text{nd},i}^{d-1}} = \sum_{t}^{T_{\text{d}}} \sum_{i=1}^{N_{\text{V}}} \Delta E_{2\text{nd},i}^t, \\ &\forall \sum_{j=1}^{N_{\text{G}}} \left(P_j^t - P_j^{t'}\right) < 0 \end{aligned} \tag{28}$$

$$\begin{aligned} &1\text{h} \cdot \sum_{t}^{T_{\text{d}}} \sum_{j=1}^{N_{\text{G}}} \left(P_j^t - P_j^{t'}\right) \\ &= \sum_{t}^{T_{\text{d}}} \sum_{i=1}^{N_{\text{V}}} \frac{\Delta E_{2\text{nd},i}^t}{\eta_{\text{PCS}} \cdot \eta_{2\text{nd},i}^{d-1}}, \\ &\forall \sum_{j=1}^{N_{\text{G}}} \left(P_j^t - P_j^{t'}\right) > 0 \end{aligned} \tag{29}$$

$$\begin{aligned} &\Delta E_{2\text{nd},1}^t : \Delta E_{2\text{nd},2}^t : \cdots : \Delta E_{2\text{nd},i}^t \\ &= C_{2\text{nd},1}^{d-1}\left(\Delta E_{2\text{nd},i}^{d-1}\right) : C_{2\text{nd},2}^{d-1}\left(\Delta E_{2\text{nd},i}^{d-1}\right) : \\ &\cdots : C_{2\text{nd},i}^{d-1}\left(\Delta E_{2\text{nd},i}^{d-1}\right) \end{aligned} \tag{30}$$

$$\Delta E_{2\text{nd},i}^d = \left(\sum_{t}^{T_d} \Delta E_{2\text{nd},i}^t\right) \Big/ N_d \tag{31}$$

$$\begin{aligned} &i \in \mathbf{S_{Batt}} \\ &= \left\{ i \,\middle|\, \begin{array}{l} C_{2\text{nd},i}^d\left(\Delta E_{2\text{nd},i}^{t_d}\right) \ge 50\% \\ \cap \left(\eta_{2\text{nd},i,t}^d\left(\Delta E_{2\text{nd},i}^{t_d}\right)\right)^2 \ge 50\% \\ \cap t + L_{1\text{st},i} \le 25\text{years} \end{array} \right\} \end{aligned} \tag{32}$$

$$\begin{aligned} &t \in \mathbf{S_{BESS}} \\ &= \left\{ t \,\middle|\, \begin{array}{l} \sum_{i=1}^{N_{\text{V}}} E_{\text{R},i} \cdot C_{2\text{nd},i}^{t_d}\left(\Delta E_{2\text{nd},i}^{t_d}\right) \ge \Delta E_{\text{BESS}} \\ \cap t \le 15\text{years} \end{array} \right\} \end{aligned} \tag{33}$$

The cost savings (22) designates the difference between the results of daily EDs with and without the operation of the BESS. Emission cost [49] is considered in (23). Power balance at each time should be maintained, as given in (24), where the WTGs have the power curve:

$$\begin{cases} 0, & 0 \le v_{\text{W}}^t < v_{CI} \\ P_{\text{WTG,max}} \cdot \dfrac{v_{\text{W}}^t - v_{\text{CI}}}{v_{\text{R}} - v_{\text{CI}}}, & v_{\text{CI}} \le v_{\text{W}}^t < v_{\text{R}} \\ P_{\text{WTG,max}}, & v_{\text{R}} \le v_{\text{W}}^t < v_{\text{CO}} \\ 0, & v_{\text{CO}} \le v_{\text{W}}^t \end{cases} \tag{34}$$

The total forecast error $P_{\text{FE}}^t$ is comprised of errors from forecast wind power and load demand. Both the errors can be regarded as uncorrelated normal distributions with mean values of zero [50], [4]. Therefore $P_{\text{FE}}^t$ follows a normal distribution with a standard deviation, i.e., $P_{\text{FE}}^t \sim N(0, \sigma_{FE}^2)$, where,

$$\sigma_{\text{FE}} = \sqrt{\left(\sigma_{\text{LE}} \cdot P_{\text{FL,max}}\right)^2 + \left(\sigma_{\text{WE}} \cdot P_{\text{WTG,max}}\right)^2} \tag{35}$$

The total daily capacity $\Delta E_{\text{BESS}}$ is capped by the total initial capacity of the BESS (25). It is fixed for charging and discharging, (26) and (27), as explained in Section IV-A. $E^t_{\text{BESS},i} < 0$ represents battery charging. The generator output is altered as load demand is changed by the operation of BESS, (28) and (29). To preserve relative capacity, battery packs with higher relative capacities should contribute more. Therefore, the energy contribution of battery packs for each time period is proportional to their remaining capacities, i.e., relative capacity at the beginning of the day (30). The average energy contribution $\Delta E^d_{\text{2nd},i}$, which is the numerator of the DOD used for calculating the daily degradation, is obtained by (31). The daily cycle number $N_d$ required by (31) can be easily counted with the proposed operating strategy. As all battery packs in the BESS are utilized in each charge and discharge operation ((30)), the cycle number for each battery pack is identical throughout as long as it is not retired from the BESS.

The operating condition for battery packs and the BESS are given by (32) and (33), respectively. Set (32) is given to check whether a battery pack should be excluded from the BESS. A single battery pack is retired if its relative capacity, efficiency or total service life reaches certain criteria. During the service life of BESS, perceivably, the number of battery packs ($N_{\text{V}}$) keeps decreasing. The BESS retires when it is unable to provide operating capacity or maximum service life is reached, (33). Criteria given in (32) and (33), such as minimum relative capacity, round trip efficiency and service life are subject to revision in case of different requirements and considerations.

Similar to the calculation of the degradation process mentioned in Section III, iterative procedures should be carried out as well for updating $C^{t_d}_{\text{2nd},i}(.)$ and $\eta^{t_d}_{\text{2nd},i}(.)$, if DoD used in battery degradation formulas is defined with the variable denominator (i.e., the actual energy capacity).

### C. SOLUTION

The procedure for solving the problem in (22)—(33) is as follows:

*Step 1*: Read system data and parameters, including EOL battery packs and wind power penetration.
*Step 2*: Set a possible value of $\Delta E_{\text{BESS}}$, (25).
*Step 3*: Randomly sample $P^t_{\text{WTG}}$ and $P^t_{\text{FE}}$.
*Step 4*: Schedule ED for day $d$ without the operation of BESS.
*Step 5*: Reform load by applying charging and discharging of BESS by (26)—(29) and share the energy contribution among battery packs using (31);
*Step 6*: Re-schedule ED with updated load by BESS operation and calculate cost savings for that day using (23).
*Step 7*: $d = d + 1$; Accumulate daily saving to total cost savings.
*Step 8*: Calculate $\Delta E^d_{\text{BESS},i}$ using (30); Update performance indices ($C^{t_d}_{\text{BESS},i}(.)$ and $\eta^{t_d}_{\text{BESS},i}(.)$); Update $\mathbf{S_{Batt}}$, retire a battery pack upon violation of (32); Update $\mathbf{S_{BESS}}$, retire the BESS upon infringement of (33).
*Step 9*: Store total cost savings for this configuration ($\Delta E_{\text{BESS}}$) upon the retirement of the BESS.
*Step 10*: Cease searching if optimal $\Delta E_{\text{BESS}}$ are found; otherwise, go to *Step 2*.

Given the nonlinearity and non-differentiability of the above problem, evolution algorithms (EAs) are suitable to avoid local optimum. In this paper, self-adaptive differential evolution (SaDE) [51] is used. To solve specific optimization problems using typical EAs, time-consuming trial-and-error searches are required for appropriate control parameters such as population **NP**, scaling factor **F**, and crossover rate **CR**. Besides, strategies and parameters are fixed once chosen but may not be effective throughout the evolution as the population may move through different regions. SaDE eliminates these drawbacks by using self-adapted trial vector generation strategies and associated control parameter values [51]–[53].

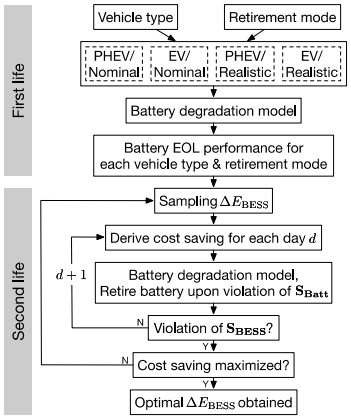


**FIGURE 3. Consolidated paradigm for the proposed evaluation framework.**

### D. CONSOLIDATED PARADIGM

Figure 3 gives the consolidated graphical paradigm for the proposed evaluation framework. It is composed of two parts: 1) Battery retirement in the first life, i.e., Section III, and 2) cost saving maximization in the second life, i.e., Section IV. In the first-life application, four scenarios are ensued from the consideration of vehicle types and retirement modes—PHEV with nominal retirement mode, EV with nominal retirement mode, PHEV with realistic retirement mode, and EV with realistic retirement mode. The outcome of the first-life modelling, i.e., battery EOL performance, is the input of the calculation of the second life. It can be seen from the figure that the battery degradation model (Section II) is applied throughout the two parts.

## V. CASE STUDY

The proposed framework is illustrated in a case study, where a 3,000 fleet (i.e., 3,000 battery packs) is recycled into a

3-generator system. Battery capacity is rated at 20.5 kWh for PHEV application and 40 kWh for the EV application. The case study is implemented in MATLAB environment.

### A. FIRST LIFE: EOL PERFORMANCE

Parameters for EOL are given as follows. For PHEV in nominal retirement mode (Section III-A), $\Delta E_{\mathrm{CD}}$ and $\Delta E_{\mathrm{CS}}$ are 11.6 kWh and 0.5 kWh, respectively, [29]. Minimum 5,000 CD and 300,000 CS cycles are required prior to nominal retirement (i.e., $N_{\mathrm{CD}}$ and $N_{\mathrm{CS}}$ in Section III-A), [29]. For EV's nominal retirement mode (Section III-B), daily travel mileages $M_i$ are randomly sampled from [54]. For realistic retirement mode (Section III-C), a probability distribution of vehicle ownership length is used [30], as is given in Appendix-C.

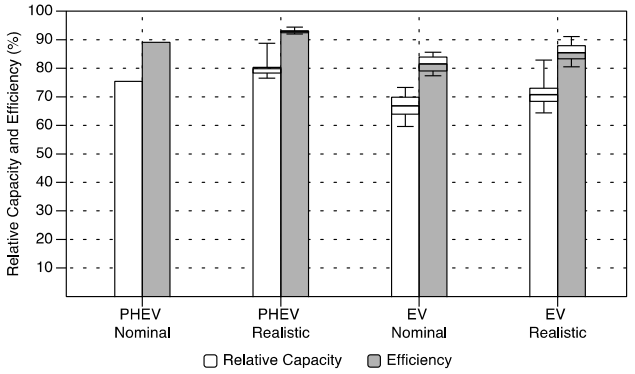


**FIGURE 4.** Average bars and box-and-whisker diagrams of EOL battery status from 3,000 vehicles.

By calculating performance degradation under the two retirement modes for both vehicle types, mean values of relative capacities and efficiencies of EOL battery packs are plotted in Figure. 4. Box plot is used to illustrate variances across 3,000 vehicles. It is most obvious to find that usage and retirement mode in the transportation sector have direct effects on EOL battery performance.

Vehicle type-wise, Figure. 4 shows that in either retirement mode EV application leads to more serious capacity fade and efficiency decay. Although battery packs for EV application are double the capacity of PHEVs', the fact that battery is the sole energy source powering EV implies deeper DoD exerted. Meanwhile, batteries in PHEV take up a supportive role, where only standard CD/CS cycles are required, (11) and (12). The EOL variance of EV battery packs can be observed in both battery retirement modes. It is because each EV's daily mileage varies, as does its $\Delta E_i$, (18).

Not only the vehicle types but their retirement modes also affect the EOL performance. On average, battery packs in realistic retirement mode are better preserved than the in nominal modes. It is because vehicles could be retired before reaching its technical EOL in reality (Section III-C and Appendix-C). Besides, EOL performance in realistic retirement modes is more widely distributed for both vehicle types. Overall, battery packs retired from PHEVs in nominal mode represent the most uniform situation whereas battery packs retired from EVs in realistic mode are most randomly distributed due to variances in both served years in vehicles and daily mileages. For degradation model used in this paper, capacity fade is more sensitive to vehicle usage than battery efficiency decay.

**TABLE 1.** Generator parameters.

| $j$ | Lower and upper bounds (MW) | $k_{0,j}$ (MMBtu) | $k_{1,j}$ (MMBtu/MW) | $k_{2,j}$ (MMBtu/MW$^2$) |
|---|---|---|---|---|
| 1 | (100, 600) | 510 | 7.92 | 0.0142 |
| 2 | (100, 400) | 310 | 7.85 | 0.00194 |
| 3 | (50, 200) | 250 | 7.50 | 0.00482 |

### B. SECOND LIFE: COST SAVINGS

Parameters of generators in the power system are provided in Table 1. Coal price is \$2.50 MMBtu and $CO_2$ price is \$4.76 MMBtu. Forecast load profile is from RTS-96 [55]. Peak load is set at 855 MW. 50 MW wind power penetration is first assumed. The wind speed follows a Weibull distribution with a shape factor of 1.72 and a scale factor of 8. The cut-in, rated and cut-out speeds of the WTGs are 3.6, 13 and 25 m/s, respectively. $\sigma_{\mathrm{LE}}$ is 0.02 per MW and $\sigma_{\mathrm{WE}}$ is 2.21 per MW installed capacity. By fitting test results from [32]–[34], [37], constants in degradation formula (7) and (8) can be obtained: $a = 2.81226 \times 10^{-5}$, $b = 2.25236$ and $c = -1.78574$ in (9); and $\alpha_1 = -3.30 \times 10^{-3}$, $\alpha_2 = -89.6$ and $\alpha_3 = -8.19 \times 10^{-3}$; $\beta_1 = -4.23 \times 10^{-2}$, $\beta_2 = 3.18 \times 10^2$ and $\beta_3 = 97.1\%$ in (10).

To have a grasp on the relationship between daily operating energy capacity ($\Delta E_{\mathrm{BESS}}$) and total cost savings. The total cost savings is first calculated with $\Delta E_{\mathrm{BESS}}$ increased step by step. PHEV battery and nominal retirement mode is chosen. Results and trend are plotted in Figure. 5.

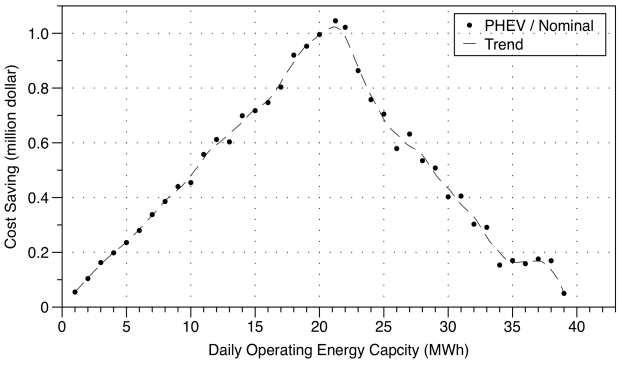


**FIGURE 5.** Total cost savings of second-life BESS with PHEV battery packs in nominal retirement mode.

As shown in the figure, the trend is that the total cost savings ascend with increased $\Delta E_{\mathrm{BESS}}$ until it reaches its peak value. According to (22), the total cost savings is affected by two factors: the difference between power outputs

of committed generators with and without BESS ($P_j^t$ and $P_j^{t'}$) and length of service life of BESS ($\mathbf{S_{BESS}}$). The larger the $\Delta E_{\text{BESS}}$ is the more is the forecast error that can be eliminated by BESS ((28) and (29)), which indicates increased daily savings. However, a higher $\Delta E_{\text{BESS}}$ leads to a higher value of $\Delta E^d_{\text{BESS},i}$, which means deeper DoD for daily operation (30). Charging and discharging with deeper DoD generally make battery performance degrade sooner, (31). Thus the BESS ends its service earlier, (32). If being operated with extremely high DoD values, e.g. when $\Delta E_{\text{BESS}} \geq 39$ MWh in PHEV-nominal scenario, the BESS retires in a short period with hardly any cost savings. In sum, the optimal daily operating energy capacity of the second-life BESS is a compromise between daily cost savings and service life takes place. For current penetration level of wind power, i.e. 5.85%, the maximum total cost savings appears when $\Delta E_{\text{BESS}}$ is around 21 MWh.

**TABLE 2. Maximum saving conditions in the four scenarios.**

| Scenarios (battery types / re-tirement mode) | $\Delta E_{\text{BESS}}$ (MWh) | Maximum total cost saving ($M) | Initial capacity (MWh) | Total cost savings per initial capacity ($M/MWh) |
|---|---|---|---|---|
| PHEV / Nominal | 21.24 | 1.03 | 41.71 | 0.025 |
| PHEV / Realistic | 20.09 | 1.56 | 46.12 | 0.034 |
| EV / Nominal | 25.07 | 1.63 | 65.39 | 0.025 |
| EV / Realistic | 28.09 | 2.17 | 72.58 | 0.030 |

Following the calculation process in Section IV-C, optimal $\Delta E_{\text{BESS}}$ values can be found for each combination of vehicle type and retirement mode. Table 2 lists maximal total cost savings for the four scenarios as well as their total EOL energy capacity, total cost savings per EOL capacity and their optimal $\Delta E_{\text{BESS}}$. It can be seen from the table that different EOL status of EV/PHEV batteries (Section V-A) go on affect their economic performance in second-life application. For same vehicle types, realistic retirement modes result in higher cost savings of the BESS than the nominal ones. In terms of total cost savings, BESS built from EV battery packs in realistic mode trumps other scenarios. However, it should be noted that an EV battery pack possesses double the energy capacity of a PHEV battery pack. The total EOL capacity is the largest, 72.58 MWh, in the EV-Realistic scenario.

To have a meaningful comparison across the four scenarios, total cost savings per EOL capacity for the second-life application are listed in Table 2. In terms of cost savings per MWh, PHEV battery in realistic mode outperforms other scenarios. The second-life BESS in the PHEV-Realistic scenario can save 0.034 $M per MWh of EOL capacity compared with 0.030 $M/MWh in the EV-Realistic scenario. Despite larger total cost savings gained, battery packs in EV-realistic scenario have inferior EOL status than in PHEV-realistic scenario. That makes EV battery packs retire sooner thus the lower cost savings per MWh. Comparing between PHEV-nominal and EV-nominal scenarios, the larger EOL EV battery capacity can interpret into more total cost savings, whereas EOL PHEV battery is better preserved. The two factors even out—resulting in the same cost savings per EOL capacity, 0.025 $M/MWh, (the first and third rows in the table).

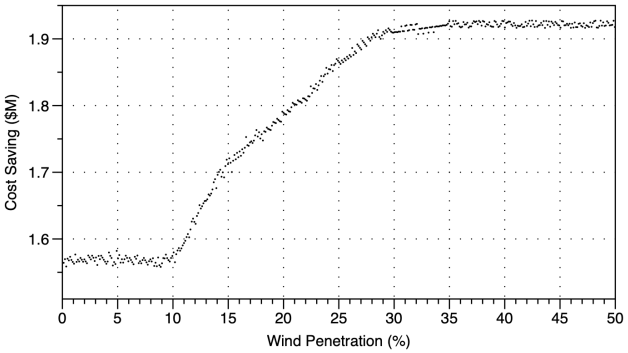


**FIGURE 6. Relationship between penetration level of WTGs and total cost savings.**

### C. SENSITIVITY STUDY

Finally, PHEV-realistic scenario is chosen to study the impact of WTG penetration levels on total cost savings. Total cost savings is re-calculated with varying WTG capacity. The amount of forecast error arises with increased wind power penetration, (37). As can be shown in Figure. 6, when the penetration level is below 10%, the total cost savings remains at a low level and insensitive to the level of penetration. When the penetration level increases from 10% to 30%, i.e., wind power accounts for more error, the total cost savings becomes sensitive to and increases with the penetration level. After penetration level reaches 30%, the cost savings still increases but the slope becomes flatter. This is because although the amount of forecast error grows with increase of penetration level, the limited energy capacity of the BESS confines further improvement of total cost savings.

**TABLE 3. Comparison of different algorithms.**

| | SaDE | GA | PSO | DE |
|---|---|---|---|---|
| Maximum cost saving ($M) | 1.56 | 1.56 | 1.56 | 1.56 |
| Computing time (s) | 458 | 621 | 592 | 560 |

### D. COMPARISON OF OPTIMIZATION ALGORITHMS

To find out the effectiveness of SaDE used in solving the optimization problem in the second-life application, classic evaluation algorithms such genetic algorithm (GA) ('ga' command in MATLAB environment), particle swarm optimization (PSO) ('particleswarm'), and differential evolution (DE) [56] are used as comparison. The same PHEV-realistic scenario is used. Wind penetration is set to the original 50 MW. The comparison results are given in Table 3. In terms of computing time, SaDE outperforms the other three. As mentioned in Section IV-C, SaDE's adaptiveness contributes to the faster convergence. On the other hand, the

default parameter setting for GA, PSO and DE might not be in favor of this specific problem. The tuning of the parameters is time-consuming. In terms of the solution, however, all the algorithms can find optimum consistently.

## VI. CONCLUSION

In this paper, a comprehensive framework evaluating second-life EV/PHEV battery in BESS application is proposed. The framework comprises of three modules: 1) Battery performance degradation model; 2) EV/PHEV battery retirement modes; and 3) evaluation for BESS application in power systems. The second-life BESS is proposed to mitigate load and wind power forecast errors. Daily operating energy capacity is optimized to maximize total cost savings of economic dispatch across the second life span of batteries.

The case study shows that the proposed framework determines the best operating strategy for the second-life BESS. The battery degradation and various first-life EOL statuses are considered. Results shows that the performance of EOL application is strongly correlated with usage and retirement mode prior to EOL. Reduced service years in vehicle application can help second-life BESS gain extra cost savings. Although EV battery packs possess larger EOL energy capacities and consequently generate more cost savings, the BESS built from retired PHEV batteries has higher cost savings per MWh. It is because in the proposed degradation model battery capacity and efficiency are better preserved in PHEV applications. Given EOL battery packs, the best second-life performance of the BESS can be obtained when a balance between short-term benefit (daily cost saving) and service years is achieved.

The proposed three-part framework can be adopted to second-life BESS applications on the generation side in the power systems. The operating strategy proposed (Section IV-A) can be used as long as there are forecast errors to be absorbed. The single decision variable ($\Delta E_{\mathrm{BESS}}$) in the optimization problem simplifies the operational process in real systems. Other degradation models for batteries [20]–[22] can also be used (in Section II) to reflect the actual battery wear and tear in specific cases.

## APPENDIX A
## CRITERIA CHECK FOR (7)

The partial derivatives of relative capacity function (7) with respect to cycle number and DoD give

$$\frac{\partial}{\partial N_C} C\,(n, D) = \frac{1}{c} \cdot \left(a \cdot 10^{b\cdot(D-1)}\right)^{-\frac{1}{c}} \cdot n^{-\frac{1}{c}-1} \tag{A1}$$

$$\frac{\partial}{\partial D} C\,(n, D) = \frac{b}{c} \cdot ln(10) \cdot (a \cdot n)^{-\frac{1}{c}} \cdot 10^{-\frac{b}{c}(D-1)} \tag{A2}$$

With given values of $a$, $b$ and $c$, for example, constants provided in Section V, the satisfaction of criteria in (2)–(6) can be easily proven with (A1) and (A2).

If $C(n, D)$ is fixed, (7) gives (A3) and the linear relationship between DoD and the logarithm of cycle number can be proven.

$$const^{+} = N_C \cdot 10^{b\cdot D} \tag{A3}$$

where $const^{+}$ designates a positive constant.

## APPENDIX B
## CRITERIA CHECK FOR (8)

By substituting (9) and (10) into (8), the second term in (8) gives

$$(\alpha_3 \cdot D - 100\% + \beta_3) + (\alpha_1 \cdot D + \beta_1) \cdot n \cdot \frac{\alpha_3 \cdot D + (\beta_3 - 100\%)}{\alpha_2 \cdot D + \beta_2} \tag{A4}$$

Provided $\alpha_3/\alpha_2$ equal to $(\beta_3 - 100\%)/\beta_2$, (8) can be expressed as:

$$\eta\,(n, D) = \alpha_3 \cdot D + \beta_3 + const \cdot (\alpha_1 \cdot D + \beta_1) \cdot n \tag{A5}$$

where $const$ denotes a constant. It can be seen from (A6) that for any cycle number a linear relationship between the efficiency and DoD exists, i.e. (10). Besides, for any DoD value the linear relationship between the battery efficiency and its cycle number can be found and its slope, $const \cdot (\alpha_1 \cdot D + \beta_1)$, increases with value of $D$. The efficiency decay criteria discussed in Section II-B are met.

## APPENDIX C
## VEHICLE OWNERSHIP LENGTH

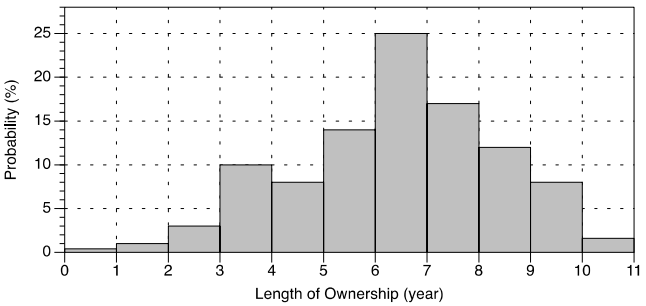


**FIGURE 7.** Length of ownership of new EV/PHEVs [30].

## REFERENCES

[1] V. V. Viswanathan and M. Kintner-Meyer, "Second use of transportation batteries: Maximizing the value of batteries for transportation and grid services," *IEEE Trans. Veh. Technol.*, vol. 60, no. 7, pp. 2963–2970, Sep. 2011.

[2] N. Jiao and S. Evans, "Business models for sustainability: The case of second-life electric vehicle batteries," *Proc. CIRP*, vol. 40, pp. 250–255, Jan. 2016.

[3] E. Martinez-Laserna, I. Gandiaga, E. Sarasketa-Zabala, J. Badeda, D.-I. Stroe, M. Swierczynski, and A. Goikoetxea, "Battery second life: Hype, hope or reality? A critical review of the state of the art," *Renew. Sustain. Energy Rev.*, vol. 93, pp. 701–718, Oct. 2018.

[4] M. A. Ortega-Vazquez and D. S. Kirschen, "Estimating the spinning reserve requirements in systems with significant wind power generation penetration," *IEEE Trans. Power Syst.*, vol. 24, no. 1, pp. 114–124, Feb. 2009.

[5] A. Assunção, P. S. Moura, and A. T. de Almeida, "Technical and economic assessment of the secondary use of repurposed electric vehicle batteries in the residential sector to support solar energy," *Appl. Energy*, vol. 181, pp. 120–131, Nov. 2016.

[6] H. Li, M. Alsolami, S. Yang, Y. M. Alsmadi, and J. Wang, "Lifetime test design for second-use electric vehicle batteries in residential applications," *IEEE Trans. Sustain. Energy*, vol. 8, no. 4, pp. 1736–1746, Oct. 2017.
[7] M. Rehme, S. Richter, A. Temmler, and U. Götze, "Second-life battery applications—Market potentials and contributions of the cost effectiveness of electric vehicles," in *Proc. 8th Wissenschaftsforum Mobilität*, Duisburg, Germany, 2017.
[8] S. Bobba, P. Andreas, F. Di Persio, M. Maarten, T. Paolo, M. Cusenza, E. Umberto, and M. Fabrice, "Sustainability assessment of second life applications of automotive batteries (SASLAB)," Joint Res. Centre, Petten, The Netherlands, Tech. Rep. JRC112543, Aug. 2018, doi: 10.2760/53624.
[9] E. Martinez-Laserna, E. Sarasketa-Zabala, I. V. Sarria, D. I. Stroe, M. Swierczynski, A. Warnecke, J. M. Timmermans, S. Goutam, N. Omar, and P. Rodriguez, "Technical viability of battery second life: A study from the ageing perspective," *IEEE Trans. Ind. Appl.*, vol. 54, no. 3, pp. 2703–2713, May/Jun. 2018.
[10] E. Cready, J. Lippert, J. Pihl, I. Weinstock, P. Symons, and R. G. Jungst, "Technical and economic feasibility of applying used EV batteries in stationary applications: A study for the DOE energy storage systems program," Sandia Nat. LAboratories, Albuquerque, NM, USA, Tech. Rep. SAND2002-4084, 2003.
[11] J. Neubauer and A. Pesaran, "NREL's PHEV/EV Li-ion battery secondary-use project," in *Proc. Adv. Automot. Battery Conf.*, Orlando, FL, USA, 2010, pp. 1–7.
[12] B. D. Williams and T. E. Lipman, "Strategy for overcoming cost hurdles of plug-in–hybrid battery in California: Integrating post-vehicle secondary use values," *Transp. Res. Rec., J. Transp. Res. Board*, vol. 2191, no. 1, pp. 59–66, Jan. 2010.
[13] J. Neubauer and A. Pesaran, "The ability of battery second use strategies to impact plug-in electric vehicle prices and serve utility energy storage applications," *J. Power Sources*, vol. 196, no. 23, pp. 10351–10358, Dec. 2011.
[14] V. Alimisis and N. D. Hatziargyriou, "Evaluation of a hybrid power plant comprising used EV-batteries to complement wind power," *IEEE Trans. Sustain. Energy*, vol. 4, no. 2, pp. 286–293, Apr. 2013.
[15] R. Faria, P. Marques, R. Garcia, P. Moura, F. Freire, J. Delgado, and A. T. de Almeida, "Primary and secondary use of electric mobility batteries from a life cycle perspective," *J. Power Sources*, vol. 262, pp. 169–177, Sep. 2014.
[16] G. Reid and J. Julve, "Second life-batteries as flexible storage for renewables energies," Bundesverband Erneuerbare Energie, Berlin, Germany, Tech. Rep., Apr. 2016. [Online]. Available: https://www.bee-ev.de/fileadmin/Publikationen/Studien/201604_Second_Life-Batterien_als_flexible_Speicher.pdf
[17] B. Williams, "Second life for plug-in vehicle batteries: Effect of grid energy storage value on battery lease payments," *Transp. Res. Rec., J. Transp. Res. Board*, vol. 2287, no. 1, pp. 64–71, Jan. 2012.
[18] M. T. Lawder, B. Suthar, P. W. C. Northrop, S. De, C. M. Hoff, O. Leitermann, M. L. Crow, S. Santhanagopalan, and V. R. Subramanian, "Battery energy storage system (BESS) and battery management system (BMS) for grid-scale applications," *Proc. IEEE*, vol. 102, no. 6, pp. 1014–1030, Jun. 2014.
[19] E. Braco, I. S. Martín, A. Berrueta, P. Sanchis, and A. Ursúa, "Experimental assessment of cycling ageing of lithium-ion second-life batteries from electric vehicles," *J. Energy Storage*, vol. 32, Dec. 2020, Art. no. 101695.
[20] S. Wang, D. Guo, X. Han, L. Lu, K. Sun, W. Li, D. U. Sauer, and M. Ouyang, "Impact of battery degradation models on energy management of a grid-connected DC microgrid," *Energy*, vol. 207, Sep. 2020, Art. no. 118228.
[21] I. Mathews, B. Xu, W. He, V. Barreto, T. Buonassisi, and I. M. Peters, "Technoeconomic model of second-life batteries for utility-scale solar considering calendar and cycle aging," *Appl. Energy*, vol. 269, Jul. 2020, Art. no. 115127.
[22] Z. Song, S. Feng, L. Zhang, Z. Hu, X. Hu, and R. Yao, "Economy analysis of second-life battery in wind power systems considering battery degradation in dynamic processes: Real case scenarios," *Appl. Energy*, vol. 251, Oct. 2019, Art. no. 113411.
[23] N. Jiao and S. Evans, "Secondary use of electric vehicle batteries and potential impacts on business models," *J. Ind. Prod. Eng.*, vol. 33, no. 5, pp. 348–354, 2016.
[24] N. Z. Xu, K. W. Chan, C. Y. Chung, and M. Niu, "Enhancing adequacy of isolated systems with electric vehicle-based emergency strategy," *IEEE Trans. Intell. Transp. Syst.*, vol. 21, no. 8, pp. 3469–3475, Aug. 2020.
[25] N. Z. Xu and C. Y. Chung, "Reliability evaluation of distribution systems including vehicle-to-home and vehicle-to-grid," *IEEE Trans. Power Syst.*, vol. 31, no. 1, pp. 759–768, Jan. 2016.
[26] C. Wan, J. Lin, W. Guo, and Y. Song, "Maximum uncertainty boundary of volatile distributed generation in active distribution network," *IEEE Trans. Smart Grid*, vol. 9, no. 4, pp. 2930–2942, Jul. 2018.
[27] Z. Cao, C. Wan, Z. Zhang, F. Li, and Y. Song, "Hybrid ensemble deep learning for deterministic and probabilistic low-voltage load forecasting," *IEEE Trans. Power Syst.*, vol. 35, no. 3, pp. 1881–1897, May 2020.
[28] S. Chai, Z. Xu, Y. Jia, and W. K. Wong, "A robust spatiotemporal forecasting framework for photovoltaic generation," *IEEE Trans. Smart Grid*, vol. 11, no. 6, pp. 5370–5382, Nov. 2020.
[29] *U.S. Advanced Battery Consortium LLC*. Accessed: Aug. 2021. [Online]. Available: http://www.uscar.org/
[30] (2016). *IHS Markit*. [Online]. Available: http://news.ihsmarkit.com/
[31] S. Saxena, C. L. Floch, J. MacDonald, and S. Moura, "Quantifying EV battery end-of-life through analysis of travel needs with vehicle powertrain models," *J. Power Sources*, vol. 282, pp. 265–276, May 2015.
[32] E. Wood, M. Alexander, and T. H. Bradley, "Investigation of battery end-of-life conditions for plug-in hybrid electric vehicles," *J. Power Sources*, vol. 196, no. 11, pp. 5147–5154, Jun. 2011.
[33] J. Belt, V. Utgikar, and I. Bloom, "Calendar and PHEV cycle life aging of high-energy, lithium-ion cells containing blended spinel and layered-oxide cathodes," *J. Power Sources*, vol. 196, no. 23, pp. 10213–10221, Dec. 2011.
[34] K. Smith, T. Markel, and A. Pesaran, "PHEV battery trade-off study and standby thermal control," in *Proc. 26th Int. Battery Seminar Exhibit*, Fort Lauderdale, FL, USA, 2009.
[35] S. Pelletier, O. Jabali, G. Laporte, and M. Veneroni, "Battery degradation and behaviour for electric vehicles: Review and numerical analyses of several models," *Transp. Res. B, Methodol.*, vol. 103, pp. 158–187, Sep. 2017.
[36] J. Li, F. Gao, G. Yan, T. Zhang, and J. Li, "Modeling and SoC estimation of lithium iron phosphate battery considering capacity loss," *Protection Control Mod. Power Syst.*, vol. 3, no. 1, p. 5, Dec. 2018.
[37] *Lithium Mobile Power: Proceedings*, 2nd ed., Knowl. Found., Brookline, MA, USA, 2008.
[38] C. Liu, J. Wang, A. Botterud, Y. Zhou, and A. Vyas, "Assessment of impacts of PHEV charging patterns on wind-thermal scheduling by stochastic unit commitment," *IEEE Trans. Smart Grid*, vol. 3, no. 2, pp. 675–683, Jun. 2012.
[39] G. A. F. Seber and C. J. Wild, *Nonlinear Regression*. New York, NY, USA: Wiley, 1989.
[40] P. Lancaster and K. Salkauskas, *Curve and Surface Fitting: An Introduction*. London, U.K.: Academic, 1986.
[41] G. J. May, A. Davidson, and B. Monahov, "Lead batteries for utility energy storage: A review," *J. Energy Storage*, vol. 15, pp. 145–157, Feb. 2018.
[42] M. Beaudin, H. Zareipour, A. Schellenberglabe, and W. Rosehart, "Energy storage for mitigating the variability of renewable electricity sources: An updated review," *Energy Sustain. Develop.*, vol. 14, no. 4, pp. 302–314, Dec. 2010.
[43] N. Z. Xu and C. Y. Chung, "Well-being analysis of generating systems considering electric vehicle charging," *IEEE Trans. Power Syst.*, vol. 29, no. 5, pp. 2311–2320, Sep. 2014.
[44] N. Z. Xu and C. Y. Chung, "Uncertainties of EV charging and effects on well-being analysis of generating systems," *IEEE Trans. Power Syst.*, vol. 30, no. 5, pp. 2547–2557, Sep. 2015.
[45] Y. J. A. Zhang, C. Zhao, W. Tang, and S. H. Low, "Profit-maximizing planning and control of battery energy storage systems for primary frequency control," *IEEE Trans. Smart Grid*, vol. 9, no. 2, pp. 712–723, Mar. 2018.
[46] P. Mercier, R. Cherkaoui, and A. Oudalov, "Optimizing a battery energy storage system for frequency control application in an isolated power system," *IEEE Trans. Power Syst.*, vol. 24, no. 3, pp. 1469–1477, Aug. 2009.
[47] G. He, Q. Chen, C. Kang, Q. Xia, and K. Poolla, "Cooperation of wind power and battery storage to provide frequency regulation in power markets," *IEEE Trans. Power Syst.*, vol. 32, no. 5, pp. 3559–3568, Sep. 2017.
[48] Y. Liu, W. Du, L. Xiao, H. Wang, S. Bu, and J. Cao, "Sizing a hybrid energy storage system for maintaining power balance of an isolated system with high penetration of wind generation," *IEEE Trans. Power Syst.*, vol. 31, no. 4, pp. 3267–3275, Jul. 2016.

[49] Z. Hu and W. T. Jewell, "Optimal power flow analysis of energy storage for congestion relief, emissions reduction, and cost savings," in *Proc. IEEE/PES Power Syst. Conf. Expo.*, Phoenix, AZ, USA, Mar. 2011, pp. 1–8.
[50] R. Doherty and M. O'Malley, "A new approach to quantify reserve demand in systems with significant installed wind capacity," *IEEE Trans. Power Syst.*, vol. 20, no. 2, pp. 587–595, May 2005.
[51] A. K. Qin, V. L. Huang, and P. N. Suganthan, "Differential evolution algorithm with strategy adaptation for global numerical optimization," *IEEE Trans. Evol. Comput.*, vol. 13, no. 2, pp. 398–417, Apr. 2009.
[52] A. K. Qin and P. N. Suganthan, "Self-adaptive differential evolution algorithm for numerical optimization," in *Proc. IEEE Congr. Evol. Comput.*, vol. 2, Sep. 2005, pp. 1785–1791.
[53] B. Mirza, M. Pant, H. Zaheer, L. Garcia-Hernandez, and A. Abraham, "Differential evolution: A review of more than two decades of research," *Eng. Appl. Artif. Intell.*, vol. 90, Apr. 2020, Art. no. 103479.
[54] (2017). *National Household Travel Survey*. [Online]. Available: http://nhts.ornl.gov/
[55] APM Subcommittee, "The IEEE reliability test system-1996," *IEEE Trans. Power Syst.*, vol. 14, no. 3, pp. 1010–1020, Aug. 1999.
[56] R. Storn and K. Price, "Differential evolution—A simple and efficient heuristic for global optimization over continuous spaces," *J. Global Optim.*, vol. 11, no. 4, pp. 341–359, 1997.

**SONGJIAN CHAI** (Member, IEEE) received the M.Sc. and Ph.D. degrees in electrical engineering from The Hong Kong Polytechnic University, Hong Kong, in 2012 and 2018, respectively. He is currently a Postdoctoral Research Fellow with Shenzhen University, Shenzhen, China. His research interests include variable renewable generation forecasting, electricity price forecasting, power system uncertainty analysis, and artificial intelligence application in power engineering.

**NING ZHOU XU** (Member, IEEE) received the B.S. and M.S. degrees in electrical engineering from the Hefei University of Technology, Hefei, China, in 2008 and 2011, respectively, and the Ph.D. degree in electrical engineering from The Hong Kong Polytechnic University, Hong Kong, in 2015. He is currently a Scientist with the Experimental Power Grid Centre (EPGC), Energy Research Institute @ NTU (ERI@N), Nanyang Technological University. His research interests include energy storage systems, demand-side management for smart grid, and the synergy between EVs and the grid.

**MING NIU** received the bachelor's degree from the Dalian University of Technology, Dalian, China, in 2010, and the M.Sc. and Ph.D. degrees from The Hong Kong Polytechnic University, Hong Kong, in 2012 and 2020, respectively. He is currently a Postdoctoral Fellow with the Electric Power Research Institute, State Grid Liaoning Electric Power Company Ltd., Shenyang, China. His research interests include renewable energy and reactive power compensation and planning, energy storage systems, power system reliability, and the synergy between EVs and grid.

**KA WING CHAN** (Member, IEEE) received the B.Sc. (Hons.) and Ph.D. degrees in electronic and electrical engineering from the University of Bath, Bath, U.K., in 1988 and 1992, respectively. He is currently an Associate Professor with the Department of Electrical Engineering, The Hong Kong Polytechnic University. His general research interests include power system stability, analysis, control, security, and optimization, real-time simulation of power system transients, distributed and parallel processing, and artificial intelligence techniques.

**CHI YUNG CHUNG** (Fellow, IEEE) received the B.Eng. (Hons.) and Ph.D. degrees in electrical engineering from The Hong Kong Polytechnic University, Hong Kong, in 1995 and 1999, respectively.

He has worked with Powertech Labs Inc., Surrey, BC, Canada; the University of Alberta, Edmonton, AB, Canada; and The Hong Kong Polytechnic University. He is currently a Professor, the NSERC/SaskPower (Senior) Industrial Research Chair in smart grid technologies, and the SaskPower Chair in power systems engineering with the Department of Electrical and Computer Engineering, University of Saskatchewan, Saskatoon, SK, Canada. He is a Member-at-Large (Global Outreach) of the IEEE PES Governing Board. He is also an Editor of IEEE TRANSACTIONS ON SUSTAINABLE ENERGY and IEEE PES LETTERS, and an Associate Editor of *IET Generation, Transmission and Distribution*. He is also an IEEE PES Distinguished Lecturer.

**HUI JIANG** received the B.S. degree from Chongqing University, Chongqing, China, in 1990, and the M.S. and Ph.D. degrees from Hunan University, Hunan, China, in 1999 and 2005, respectively, all in electrical engineering. From 2005 to 2006, she was a Visiting Scholar with Brunel University, London, U.K. She is currently a Professor with Shenzhen University. Her interests include power system economics and smart grid operation.

**YUXIN SUN** is currently pursuing the bachelor's degree with the Department of Electrical Engineering and Electronics, University of Liverpool, Liverpool, U.K.